J. Space Technol. Appl. 4(3), 185-198 (2024)
https://doi.org/10.52912/jsta.2024.4.3.185

우주기술과 응용
Journal of Space Technology and Applications
pISSN 2765-7469 eISSN 2799-3213

기술논문

Development of Adaptive Optics System for the Geochang 100 cm Telescope

Hyung-Chul Lim[1†], Francis Bennet[2], Sung-Yeol Yu[1], Ian Price[2], Ki-Pyoung Sung[1], Mansoo Choi[1]

[1]Korea Astronomy and Space Science Institute, Daejeon 34055, Korea
[2]Research School of Astronomy and Astrophysics, Australian National University, Canberra 0200, Australia

Abstract

Korea Astronomy and Space science Institute (KASI) partnered with the Australian National University (ANU) to develop the adaptive optics (AO) system at the Geochang observatory with a 100 cm optical telescope for multiple applications, including space geodesy, space situational awareness and Korean space missions. The AO system is designed to get high resolution images of space objects with lower magnitude than 10 by using themselves as a natural guide star, and achieve a Strehl ratio larger than 20% in the environment of good seeing with a fried parameter of 12–15 cm. It will provide the imaging of space objects up to 1,000 km as well as its information including size, shape and orientation to improve its orbit prediction precision for collision avoidance between active satellites and space debris. In this paper, we address not only the design of AO system, but also analyze the images of stellar objects. It is also demonstrated that the AO System is achievable to a near diffraction limited full width at half maximum (FWHM) by analyzing stellar images.

Keywords: adaptive optics, atmospheric turbulence, natural guide star, space situational awareness

Received: May 10, 2024
Revised: July 2, 2024
Accepted: July 23, 2024

†Corresponding author :
Hyung-Chul Lim
Tel : +82-42-865-3235
E-mail : hclim@kasi.re.kr

ORCID

Hyung-Chul Lim
https://orcid.org/0000-0001-5266-1335
Francis Bennet
https://orcid.org/0000-0001-9797-1724
Sung-Yeol Yu
https://orcid.org/0000-0002-9571-1985
Ian Price
https://orcid.org/0000-0002-5009-9155
Ki-Pyung Sung
https://orcid.org/0000-0003-2639-4127
Mansoo Choi
https://orcid.org/0000-0003-2004-2972

1. INTRODUCTION

Space debris has been a potential threat to space missions and human space activities because its collision probability is increasing due to the exponential growth of space debris population. The spatial density of orbiting objects is so sufficiently high that a collision would cause a collisional cascading problem known as Kessler Syndrome [1] unless any action is taken to decrease the amount of space debris, such as anti-collision maneuver and space debris removal.

The two line elements (TLE) catalogue of space debris is generated and maintained by the US Air Force using radar and passive optical tracking data for various orbit propagation tasks. But it is often found that the TLE catalogue does not provide the required orbit accuracy for the space debris collision warnings, for example, the collision between the Iridium 33 satellite and the defunct Cosmos 2,251 on February 10, 2009.

Improving the orbital prediction accuracy is necessary to prevent collision against space debris, or to avoid unnecessary anti-collision maneuvers of operational spacecrafts.

The accurate orbital prediction is achievable using the combination of optical and laser tracking data obtained even from a single station through the estimation of ballistic coefficients [2–5]. In contrast to the satellite laser ranging (SLR) of cooperative targets with laser retro-reflector array (LRA), the laser ranging of space debris requires higher laser power because of low reflectivity of uncooperative target without LRA. The ranging precision is in range of 30 cm to 230 cm [6–8], resulting from space debris size and large laser pulse width of nanoseconds. Even though the debris laser ranging provides accurate measurements with one or two orders of magnitude better than the radar and passive optical tracking system, the dynamic model should take into account the debris characteristics such as size, shape and orientation information in order to improve the orbital prediction precision. The debris characteristics will influence the accurate orbital prediction as non-gravitational perturbations such as atmospheric drag and solar radiation pressure are heavily influenced by them [9]. They are available from high resolution images by ground-based optical telescope. But the image is highly distorted by atmospheric turbulence to such an extent that the image may not be often recognizable.

Adaptive optics (AO) is a technology to improve the image quality by compensating the global tilt and the local phase fluctuations for the incoming wavefronts distorted by atmospheric turbulence. It provides the high resolution image of space objects including active satellites and space debris, close to the diffraction limit of an optical telescope. Currently, AO technologies have been increasingly used for space situational awareness (SSA), particularly in the field of the space object imaging and identification, space debris laser tracking (DLT) and space debris removal [10–15].

Korea Astronomy and Space science Institute (KASI) established the space optical and laser tracking (SOLT) system at Geochang observatory for space geodesy, SSA and Korean space missions [16]. Fig. 1 shows the external view of Geochang observatory located at 950 m above the sea level. The SOLT system consists of three systems sharing an optical telescope with 100 cm clear aperture: SLR, AO, and DLT. The AO system is designed to be capable of imaging the space objects brighter than 10 magnitude using space objects as a natural guide star. It will provide space object information such as size, shape and orientation which are available from the characterization and identification process based on the AO high resolution imagery. To develop the AO system KASI specified the site characteristics, design performance, and some critical parameters. The Australian National University (ANU) designed, build, and installed the AO system including initial operations to successfully demonstrate its capabilities. In this paper, we present the design and development of AO system which was implemented at the Geochang observatory. In addition, it is demonstrated that the AO system provides the

Fig. 1. Drone photo of Geochang observatory located at Gamak mountain.

good stellar images with a near diffraction limit and shows good performance in terms of the full width at half maximum (FWHM).

2. DESIGN OF ADAPTIVE OPTICS SYSTEM

Light propagation through the atmosphere is inevitably aberrated by atmospheric turbulence which degrades image quality obtained with a ground-based optical telescope. The AO measures the distorted wavefront using a wavefront sensor (WFS), and then compensates the atmospheric turbulence in real time by controlling an active optical element such as a tip-tilt mirror and deformable mirror (DM) in order to provide the high quality image of space objects. As shown in Fig. 2 illustrating the AO operational principle, the AO system consists of a WFS, a DM, a control system and an imaging camera. A dichroic beamsplitter is used to split the incoming beam into two beams, depending on the wavelength and then transmit the beam to the WFS and the imaging camera, so that wavefronts are measured at the same time when images are taken.

The AO design is seriously determined by the telescope size and atmospheric conditions at the site. So the AO system of the Geochang station is designed to image the space objects brighter than 10 magnitude up to 1,000 km using the 100 cm telescope, and achieve a Strehl ratio larger than 20% in the environment of good seeing with coherence length (or Fried parameter) of 12 to 15 cm and wind speed of 8 to 10 m/s. The AO system is also designed to use the sunlight of the visible wavelength range reflected from space objects as the natural guide star light for the wavefront measurement, and the infrared wavelength range for imaging.

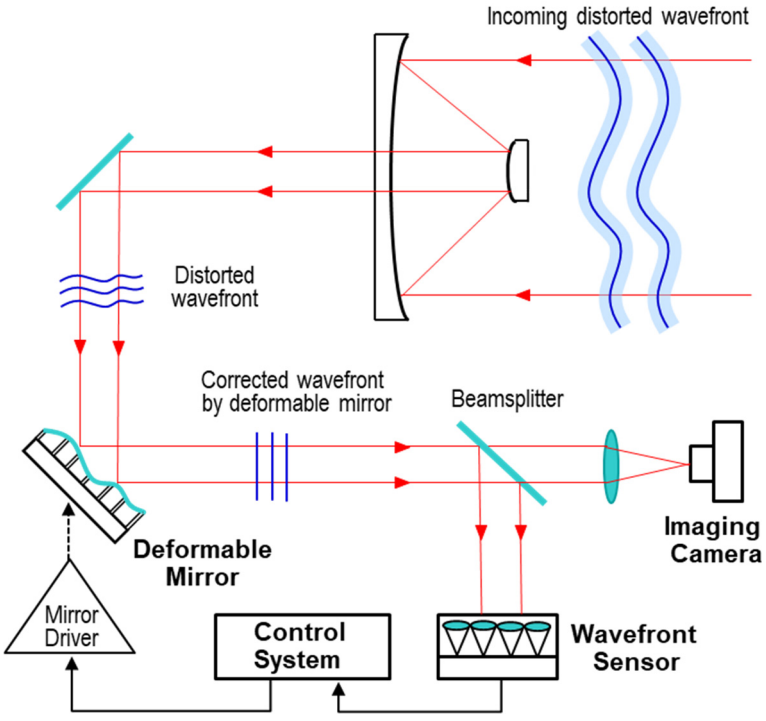

Fig. 2. Operational principle of adaptive optics (AO) system.

2.1 Optical Design

Light from the optical telescope is directed to one of three systems (i.e., SLR, AO, and DLT systems) by switching a Coudé mirror inside the telescope pedestal. The SLR, AO, and DLT systems are installed on an optical bench in a temperature and humidity controlled Coudé room, respectively. Seven Coudé mirrors including the primary and secondary mirrors are coated against a high power laser for DLT operation. The optical telescope is designed using a parabolic primary mirror with 100 cm clear aperture and focal ratio of f/1.5, and a parabolic secondary mirror with 25 cm clear aperture. It provides a diffraction limit of 0.18 arcseconds at 850 nm wavelength which will be able to resolve features 85 cm in size for space objects at the distance range of 1,000 km.

Fig. 3 shows the optical schematic of AO system. The collimated beam with 250 mm diameter via Coudé path is reduced into 12.5 mm by an on-axis beam expander with a f/5.3 parabolic mirror and a collimating lens, and then reflected off the DM to the dichroic beamsplitter. The light is split by the beamsplitter, making the light of wavelengths from 450–800 nm pass to the WFS, and the light of wavelengths from 800–1,000 nm reflected to the imaging camera. The WFS has also a beam expander which converts the beam from 12.5 mm to 2.5 mm, which consists of three lenses, the first two forming a compound lens to adjust the precise size of the beam. The pupil is also relayed, making the DM conjugate to the lenslet array, which also corresponds to the telescope pupil. A calibration source is also inserted onto the AO optical bench to calibrate the AO

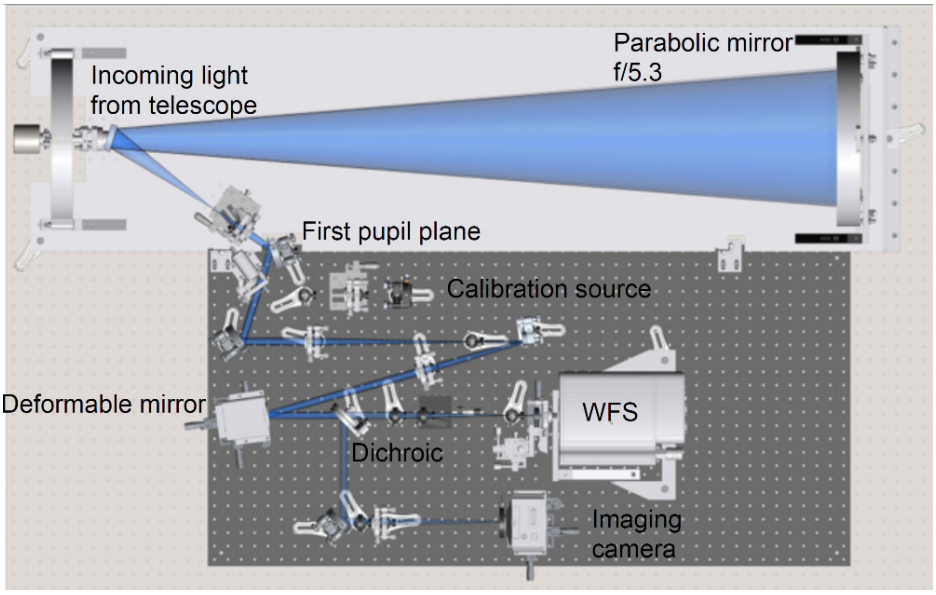

Fig. 3. Optical design of adaptive optics (AO) system.

system setup and to optimize the performance between the DM and the WFS, which is applicable by a mechanical flip mirror.

2.2 System Instrumentation

The AO system uses a Shack-Hartman WFS consisting of a lenslet array with 8 × 8 subapertures and a OCAM2K camera available from First Light Imaging which uses an electron-multiplying charged-coupled device (EMCCD) sensor. The lenslet array has a pitch of 300 μm and a radius of curvature of 9.5 mm which achieves a pixel scale of 0.6 arcseconds per pixel. The OCAM2K camera has 240 × 240 pixels and can be operated up to 2,067 frame per second (fps) with sub-electron readout noise (< 0.3 e– at 2,000 fps and 600 multiplication gain). It also offers an extremely low latency allowing high speed operation: 43 μs between exposure and first pixel availability. The OCAM2K camera is cooled to −45℃ with liquid cooling and a thermoelectric cooler in order to prevent sensor damage by over illumination, and also has firmware protections to minimize the risk of over illumination.

The DM is an ALPAO DM97-15 which has 97 actuators, maximum pupil diameter of 13.5 mm, a large stoke of actuators in range of up to 30 μm for tip-tilt, and large bandwidth up to 2 kHz with 45 degrees of phase lag. The large stoke and bandwidth allows the AO system to compensate atmospheric turbulence without a fast steering or tip-tilt mirror for high-order aberration correction. The actuators are arranged in a 11 × 11 grid with a spacing of 1.5 mm. With a clear aperture of 13.5 mm, only 9 × 9 actuators are in the visible area, whereas the outer ring of actuators are extrapolated for stability of the mirror edge.

The imaging camera is fed with corrected wavefronts in real time, which includes the camera optics and imaging detector. The Raptor Falcon EM285-CL of imaging camera has a EMCCD sensor with 1,004 × 1,002 pixels, 64 mm^2 of active area, and can be operated up to 30 Hz (Table 1). The image derotation is done by post-processing software combined with lucky imaging and imaging data so that a mechanical derotation device is not necessary. Fig. 4 shows the AO system established at Geochang observatory.

2.3 Close Loop Wavefront Correction

The AO closed loop control system hosted on an real-time computer (RTC) ties together the WFS, DM, imaging camera, and telescope offsets to maintain satellite tracking and perform AO correction (Fig. 5). A custom software server controls all electronic components of the AO system including LED calibration source with variable

Table 1. Specifications of adaptive optics (AO) system

Instruments	Parameter	Value
WFS	Camera model	OCAM2K
	Number of subapertures	8 × 8
	Wavelength range	450–800 nm
	Sampling frequency	≤ 2,067 Hz
	Read-out noise	0.3 e−
	Slope computation	Center of gravity
DM	Model	DM97-15
	Number of actuators	97
	Wavefront tip/tilt stroke (PtV)	40–60 μm
	Bandwidth	≤ 2 kHz
Imaging camera	Model	Falcon EM285-CL
	Wavelength range	800–1,000 nm
	Number of pixels	1,004 × 1,002
	Pixel size	8 μm × 8 μm
	Frame rate	30 Hz
Control	Gain	User selectable
	Mode	Zonal
	Correction rate	≤ 2 kHz

WFS, wavefront sensor; DM, deformable mirror.

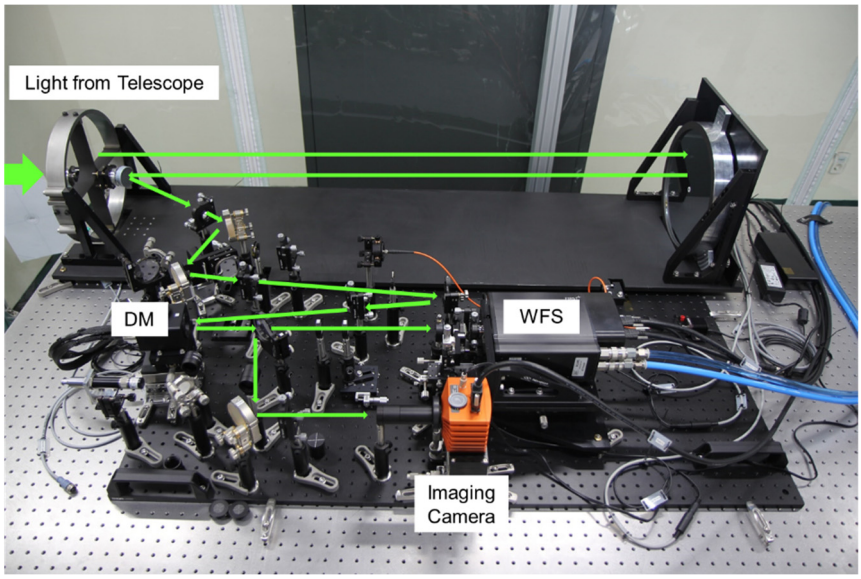

Fig. 4. Adaptive optics (AO) system established at Geochang observatory. DM, deformable mirror; WFS, wavefront sensor.

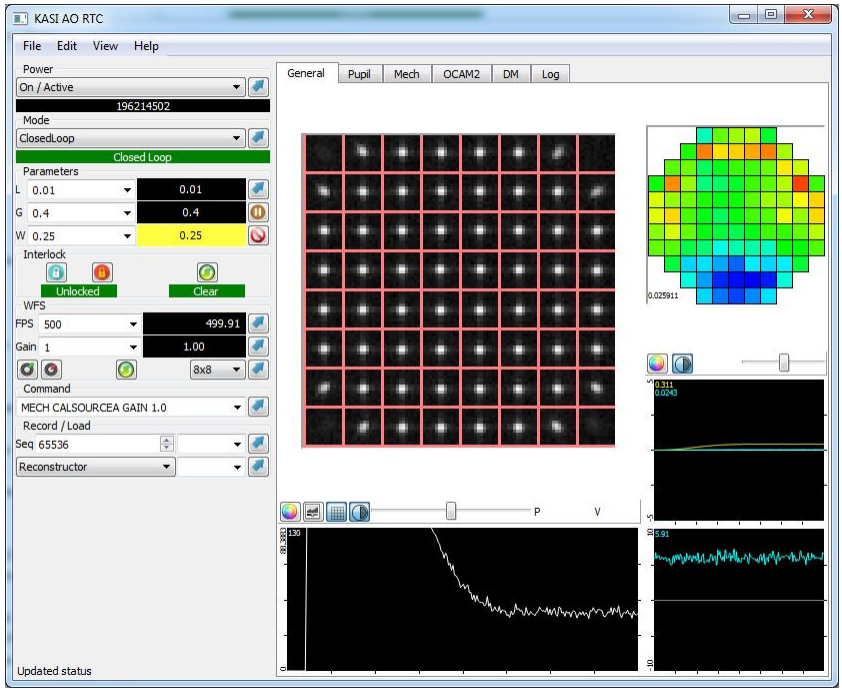

Fig. 5. Graphical user interface (GUI) of real-time computer (RCT) when the loop is closed and the wavefront is well corrected.

brightness, flip mirror to switch between calibration and sky, imaging and WFS cameras, DM, and telescope control.

Safety interlocks for several systems are controlled by the RTC to assist the controller in avoiding damage to AO system components. Safety is critical for the continued

operation of the DM, and WFS and imaging cameras. The DM has limits on the inter-actuator stroke which must be considered in the control loop as it is an additive process, with each step incrementing on the last. Constraints are required therefore to make sure that the representation of the DM shape in the RTC for computation of the next frame is sufficiently close to the actual DM shape, as there is no electrical feedback from the DM control electronics.

Both cameras are EMCCD, which uses a high-voltage gain amplifier to increase the signal without adding additional readout noise to the camera. If over-exposed, these gain regions can be damaged by the high current throughput, and so over-illumination can be dangerous. To assist the operator in recognizing these dangers and possible situations where damage may occur, the RTC has interlocks on the control loop gain, and EM gain of the cameras. If a dangerous situation should occur such as loss of light from subapertures due to sudden misalignment or something blocking the beam, the control loop will be suspended. If either of the cameras should receive too much light, their gain will be set to 1 to minimize the danger. These interlocks are reported in the log and must be manually reset using the graphical user interface (GUI) to continue operation. During normal operation they are typically not triggered.

Data from the WFS is decoded and split into subapertures, and calibrated for camera bias and sky background. A centre of gravity computation is done on each subaperture to determine the slope. A software-based windowing mechanism allows the system to increase its performance when the seeing is good: the controller can select to narrow down the subapertures, reducing the number of pixels in each subaperture. This reduces the background noise otherwise present when using a centre of gravity calculation. This parameter is user-selectable in real-time, allowing the controller to optimize the AO system performance based on current atmospheric conditions.

DM commands are computed from an interaction matrix using the computed slopes. Commands are sent to the DM on a zonal basis, where each actuator is commanded individually. The closed loop control system uses a leaky integrator with user selectable gain and leak values, and includes spatial filtering to prevent the DM from entering modes which are not measureable by the WFS. Tip-tilt modes are filtered on a temporal basis and fed to the telescope control system to maintain pointing towards the observation target.

The AO system design includes a remote controllable flip mirror and variable intensity LED source to provide hands-off calibration of the system (that is: no-one needs to enter the laboratory and physically touch anything to perform the calibration). These calibration runs can be used to track alignment changes over time, aid in aligning the system, and provide up-to-date interaction matrix for optimize the system performance.

3. RESULTS AND PERFORMANCE ANALYSIS

The performance of AO system implemented at the Geochang observatory with a 100 cm optical telescope is analyzed using two stellar sources, faint and bright stars. The astronomical seeing of general sky conditions at the Geochang observatory is in the range of 2 to 3 arcseconds, which is dependent on the degree of atmospheric turbulence.

The AO system was tested for the faint and bright stars with the visible magnitude of 9.4 (V band) and 1.25 (V band), in order to analyze the AO performance depending on the brightness of a natural guide star. Figs. 6 and 7 show the stacked images of the faint and bright stars, without the AO correction and with the AO correction, respectively. The images are obtained using the lucky imaging algorithm in which the image rotation motion can be also removed. It is shown from Fig. 6 and 7 that the AO correction makes the stellar light to be concentrated in very small number of pixels, compared with stellar images without the AO correction. The diffraction ring is shown in the right images obtained by the AO correction and the lucky imaging algorithm.

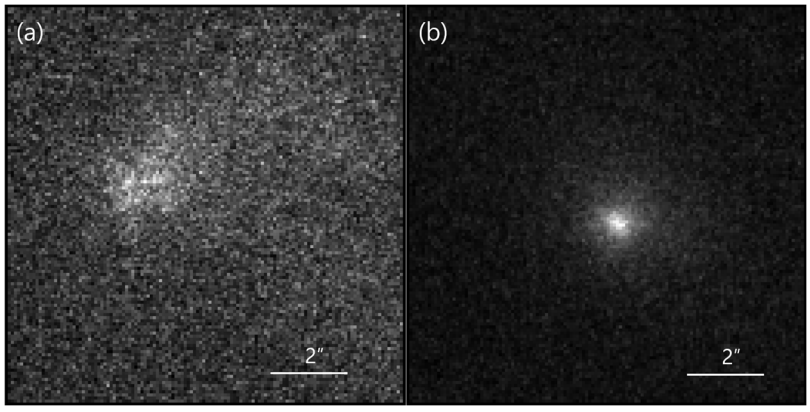

Fig. 6. Stacked image of the stellar object with visible magnitude of 9.4, (a) for without the adaptive optics (AO) correction and (b) with the AO correction.

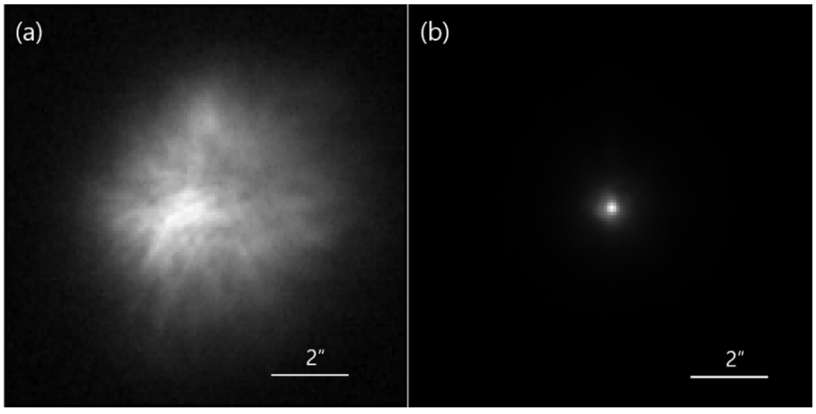

Fig. 7. Stacked images of the stellar object with visible magnitude of 1.25, (a) without the adaptive optics (AO) correction and (b) with the AO correction.

Fig. 8 shows the image profiles with FWHM of a stacked image with the AO correction for the faint and bright stars. The x-axis means the number of pixels and the y-axis is the intensity which also depends on the camera gain. For the faint star, FWHM of the stellar profile is 2.2 arcseconds without the AO correction, whereas FWHM is 0.45 with the AO correction. In the case of the bright star, FWHMs of the stellar profile are 1.9 arcseconds without the AO correction and 0.38 arcseconds with the AO correction, respectively. It was demonstrated from the stellar observations that the AO system at Geochang observatory could mitigate effectively the atmospheric turbulence and result in the good stellar images, by approximately 5 times improvement in terms of FWHM of the stellar image profile.

It is necessary to analyze the AO performance in terms of a single image enhancement, instead of a stacked image. Fig. 9 shows the image profiles with the largest and smallest FWHM of single images with the AO correction for the bright star, which are used in the stacked image shown in Fig. 7(b). In the case of the faint star, it was impossible to obtain FWHM value from a single image due to the weak stellar light. The single images with the AO correction have FWHMs in range of 0.28 arcseconds to 0.40 arcseconds, in which most FWHMs are smaller than the stacked image. In general, FWHM of a stacked image is larger than a single image because many images are accumulated in a single stacked image.

4. CONCLUSION

KASI in partnership with ANU developed the AO system which is capable of imaging the space objects up to the altitude of 1,000 km by using themselves as a natural guide

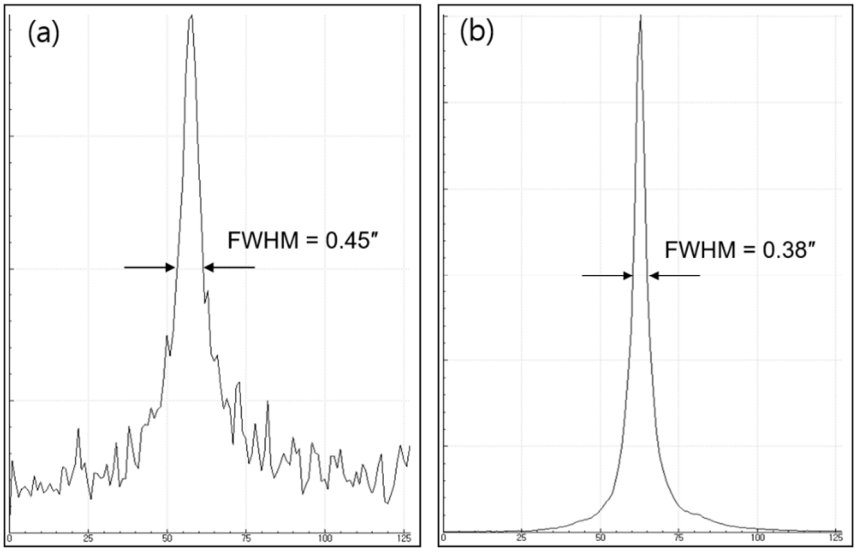

Fig. 8. Full width at half maximum (FWHM) of a stacked image with the adaptive optics (AO) correction for the stellar objects with visible magnitude of (a) 9.4 and (b) 1.25.

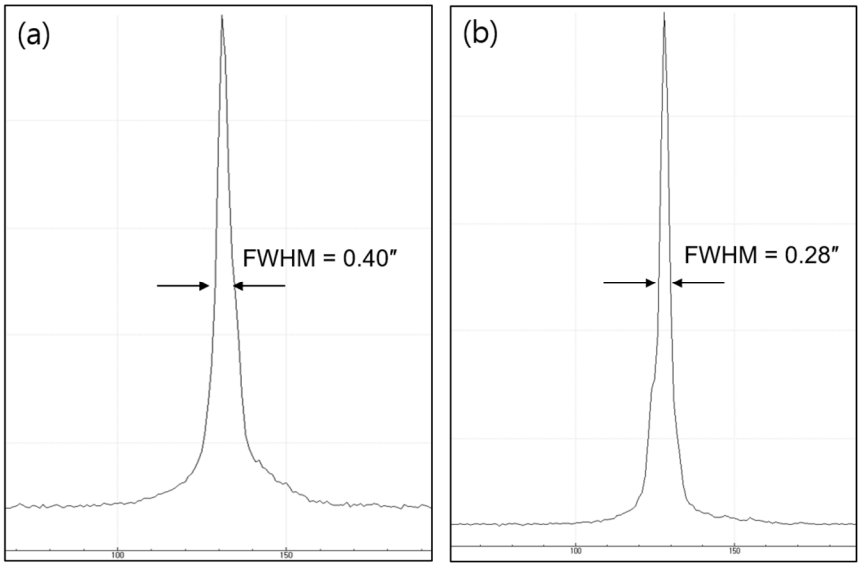

Fig. 9. Full width at half maximum (FWHM) of a single image with the adaptive optics (AO) correction for the stellar object with visible magnitude of 1.25, showing (a) largest FWHM and (b) smallest FWHM values.

star. The AO system was implemented at the Geochang observatory with the optical telescope of 100 cm clear aperture for SSA and Korean space missions.

In this study, the AO system was addressed and its performance was also demonstrated using two stellar sources, faint and bright stars. The AO system is designed to use the sunlight reflected by space objects as a natural guide star, measure the distrorted wavefronts with the WFS and then correct them using the DM with the large stroke, without the tip-tilt mirror. It consists of the WFS with 8 × 8 subapetures, the DM with 97 actuators and the closed loop control system with the correction rate up to 2 kHz. It was shown from stellar observation that the AO system was able to provide the high resolution image near the diffraction limit and then improve significantly the optical performance in terms of the FWHM of stellar profile, approximately 5 times improvement.

Recently, laser communication and quantum key distribution between ground stations and satellites has gained more attractions due to the higher data rate and secure communication, in which the mitigation of atmospheric turbulence plays an important role for the higher reliability. Thus, it is expected that the AO technologies will be also utilized for the satellite laser communication and quantum key distribution.

ACKNOWLEDGMENTS

This work was supported by the Korea Astronomy and Space Science Institute through the project of "Development of 30 km Long-range Free-space Quantum Key Distribution

System and Core-technologies for Satellite Quantum Secure Communication" funded by the Ministry of Science and ICT (MSIT) of the Korean government.

References

1. Kessler DJ, Cour-Palais BG, Collision frequency of artificial satellites: the creation of a debris belt, J. Geophys. Res. 83, 2637-2646 (1978). https://doi.org/10.1029/JA083iA06p02637
2. Bennett JC, Sang J, Smith CH, Zhang K, Accurate orbit predictions for debris orbit manoeuvre using ground-based lasers, Adv. Space Res. 52, 1876-1887 (2013). https://doi.org/10.1016/j.asr.2013.08.029
3. Sang J, Bennett JC, Achievable debris orbit prediction accuracy using laser ranging data from a single station, Adv. Space Res. 54, 119-124 (2014). https://doi.org/10.1016/j.asr.2014.03.012
4. Sang J, Bennett JC, Smith C, Experimental results of debris orbit predictions using sparse tracking data from Mt. Stromlo, Acta Astronaut. 102, 258-268 (2014). https://doi.org/10.1016/j.actaastro.2014.06.012
5. Bennet F, D'Orgeville C, Price I, Rigaut F, Adaptive optics for satellite imaging and space debris ranging, Proceedings of the Advanced Maui Optical and Space Surveillance Technologies Conference, Hawaii, HI, 15-18 Sep 2015.
6. Zhang ZP, Yang FM, Zhang HF, Wu ZB, Chen JP, et al., The use of laser ranging to measure space debris, Res. Astron. Astrophys. 12, 212-218 (2012). https://doi.org/10.1088/1674-4527/12/2/009
7. Kirchner G, Koidl F, Friederich F, Buske I, Völker U, et al., Laser measurements to space debris from Graz SLR station, Adv. Space Res. 51, 21-24 (2013). https://doi.org/10.1016/j.asr.2012.08.009
8. Sun H, Zhang HF, Zhang ZP, Wu B, Experiment on diffuse reflection laser ranging to space debris and data analysis, Res. Astron. Astrophys. 15, 909-917 (2015). https://doi.org/10.1088/1674-4527/15/6/013
9. Fruh C, Kelecy TM, Jah MK, Coupled orbit-attitude dynamics of high area-to-mass ratio (HAMR) objects: influence of solar radiation pressure, Earth's shadow and the visibility in light curves, Celest. Mech. Dyn. Astron. 117, 385-404 (2013). https://doi.org/10.1007/s10569-013-9516-5
10. Mason J, Stupl J, Marshall W, Levit C, Orbital debris–debris collision avoidance, Adv. Space Res. 48, 1643-1655 (2011). https://doi.org/10.1016/j.asr.2011.08.005
11. Rubenchik AM, Fedoruk MP, Turitsyn SK, The effect of self-focusing on laser space-debris cleaning, Light Sci. Appl. 3, e159 (2014). https://doi.org/10.1038/lsa.2014.40
12. Bennett JC, Sang J, Smith C, Zhang K, An analysis of very short-arc orbit determination for low-Earth objects using sparse optical and laser tracking data, Adv. Space Res. 55, 617-629 (2015). https://doi.org/10.1016/j.asr.2014.10.020

13. Bennet F, Price I, Rigaut F, Copeland M, Satellite imaging with adaptive optics on a 1 m telescope, in Advanced Maui Optical and Space Surveillance Technologies Conference, Hawaii, HI, 20-23 Sep 2016.
14. Copeland M, Bennet F, Zovaro A, Riguat F, Piatrou P, et al., Adaptive optics for satellite and debris imaging in LEO and GEO, in Advanced Maui Optical and Space Surveillance Technologies Conference, Hawaii, HI, 20-23 Sep 2016.
15. Grosse D, Bennet F, Copeland M, d'Orgeville C, Rigaut F, et al., Adaptive optics for satellite imaging and earth based space debris manoeuvres, in 7th European Conference on Space Debris, Darmstadt, Germany, 18-21 Apr 2017.
16. Lim HC, Sung KP, Yu SY, Choi M, Park E, et al., Satellite laser ranging system at Geochang station, J. Astron. Space Sci. 35, 253-261 (2018). https://doi.org/10.5140/JASS.2018.35.4.253

Author Information

Hyung-Chul Lim hclim@kasi.re.kr

Dr. Hyung-Chul Lim received the Ph.D. degree in aerospace engineering from KAIST in Daejeon, Korea. He has been working at KASI in the same 9 since 2000. During he stayed at KASI, he also worked as a visiting scientist at NASA Goddard Space Flight Center from 2009 to 2010, and as a professor at UST in Daejeon from 2015 to 2020. His research areas include laser remote sensing for space applications, and beam steering technologies and atmospheric turbulence mitigations for both space laser and quantum communications.

Sung-Yeol Yu kpsung@kasi.re.kr

Mr. Sung-Yeol Yu received a master's degree in space science from the Department of Astronomy and Space Science at Chungnam National University. He has been working on the optical system of the satellite laser tracking system at the Korea Astronomy and Space Science Institute since 2018, and is currently carrying out operational and research works on the optical system of Sejong and Geochang Satellite Laser Observatories.

Francis Bennet francis.bennet@anu.edu.au

Associate Professor Francis Bennet is a researcher of optical instrumentation at the Australian National University. He has expertise in adaptive optics for astronomical instrumentation, space situational awareness, and laser communication, with a focus on taking world leading ANU quantum communications experiments from the lab to space. Assoc. Prof. Bennet is leading the ACT Node of an Australian optical communication network, as well as development of a satellite to test quantum communication between space and the ground.

Ian Price ian.price@anu.edu.au

Ian Price is a software engineer at the Advance Instrumentation Technology Center within the Research School of Astronomy & Astrophysics at the Australian National University. His interests include Linux-based real-time control systems and he has extensive experience designing, developing and commissioning adaptive optics systems.

Author Information

Ki-Pyoung Sung kpsung@kasi.re.kr

Mr. Ki Pyoung Sung received the M.S degree in the department of computer engineering from Chungnam National University. He is currently working at Space Hazard Surveillance Center of KASI from 2018. He developed the operation system of Sejong and Geochang satellite laser ranging (SLR) stations. His research interests include technologies related to SLR, free space optical laser communication and national defense.

Mansoo Choi cmsoo@kasi.re.kr

Dr. Mansoo Choi received his Ph.D. in Control and Navigation from the Department of Electronic Engineering at Chungnam National University. Since 2008, he has been conducting research related to the operation and utilization of satellite navigation systems at the Korea Astronomy and Space Science Institute. He is currently engaged in research on satellite laser ranging systems and space defense at the Center for Space Situational Awareness.